A Diffeomorphic Mapping Based Characterization of Temporal Sequences: Application to the Pelvic Organ Dynamics Assessment

Mehdi Rahim, Marc-Emmanuel Bellemare, Rémy Bulot, Nicolas Pirró

Journal of Mathematical Imaging and Vision manuscript No.
(will be inserted by the editor)

A Diffeomorphic Mapping Based Characterization of Temporal Sequences : Application to the Pelvic Organ Dynamics Assessment

Mehdi Rahim · Marc-Emmanuel Bellemare · Rémy Bulot · Nicolas Pirró

Received: date / Accepted: date

Abstract In various imaging applications, shape variations are studied in order to define the transformations involved or to quantify a distance between each change performed. Regardless of the way the shapes may be extracted, with 2D imaging, shapes concern essentially curves or sets of points depending on the available data. Wether time is related to the shape variations or not, one can consider a set of shapes as the observation of the temporal evolution of an initial shape. In this context, we present a methodology aiming at quantifying the evolution of a set of contours without landmarks. Our characterization of temporal sequences is based on the large deformation diffeomorphic mapping paradigm and the shape representation based on currents, which allow both to propose a shape metric and a curve matching of the timed variations. Then, mechanics related features are extracted as they are physically meaningful and quite painless understandable.
In this paper, the process is applied within the scope of a pelviperineology study. Available clinical diagnoses are combined with statistical analysis to show the soundness of the approach. Indeed, pelvic floor disorders are characterized by abnormal organ descents and deformations during abdominal strains. As they are soft-tissue organs, the pelvic organs have no fixed landmarks, in addition to wide shape differences. Routinely used, 2D sagittal MRI sequences are segmented to provide the contour sets from which the characterization should highlight pelvic organ behaviors. We believe that a statistical analysis of these behaviors on several dynamic MRI sequences could help to a better understanding of the pelvic floor pathophysiology. The methodology is applied on a dataset of 30 patients with different clinical diagnoses. Some promising results are presented, where the pathology detection capability of the deformation features is assessed, and the principal organ dynamics modes are computed, through an inter-patient analysis. Also, an organ parcellation is proposed thanks to the local deformation analysis, it identifies spatial references which are clinically relevant.

Keywords currents · LDDMM · deformation analysis · computational anatomy · dynamic MRI · pelvic dynamics

This work is part of the **MoDyPe** project (http://modype.lsis.org) supported by the French National Research Agency (ANR) under reference "ANR-09-SYSC-008".

M. Rahim (✉)
LSIS UMR CNRS 7296
Aix-Marseille University
Domaine universitaire de Saint-Jérôme
13397, Marseille, France
Tel.: +33-491-056035
Fax: +33-491-056033
E-mail: mehdi.rahim@lsis.org

M.-E. Bellemare · R. Bulot
LSIS UMR CNRS 7296
Aix-Marseille University
E-mail: marc-emmanuel.bellemare@lsis.org
Tel.: +33-491-056024

N. Pirró
Digestive Surgery Departement
La Timone Hospital
13385, Marseille, France

1 Introduction

Pelvic floor disorders cover pathologies that associate a loss of normal anatomical link of pelvic organs, leading to altered anorectal or urogenital functions and degraded life quality. Those pathologies result from various factors such as aging, pregnancy, childbirth, obesity, injuries, or a combination of them. They mainly concern a growing population of old people, 60% of 60 years old women are concerned by those troubles, and according to a survey of 4000 women,

one women in three has a pelvic floor disorder [28]. They are considered as a public health issue in several countries. Besides the clinical examination, the pelvic dynamic MRI is a recommended tool for the clinical diagnosis of these pathologies [17], [38]. Thanks to its appreciable contrast, dynamic MRI allows to qualitatively assess the behavior of the main pelvic organs (bladder, uterus-vagina, rectum) during an abdominal strain. The pelvic cavity has the property to include structures of different nature (muscles, ligaments, bones, ...), where different interactions happen, producing diverse functions, such as urination, defecation, etc. Figure 1(a) depicts the main pelvic organs on a sagittal MRI frame. The pelvic viscera (bladder, uterus, vagina, rectum) are located between the pubic symphysis in front, and the sacrum in behind. They are linked with musculo-aponeurotic structures such as the levator ani whose role is essential in the pelvic floor activity. According to radiologists, the most relevant observation of the pelvic dynamics is done within the median sagittal plane. Even though partial, this latter is the only dynamic acquisition available in clinical routine. The movements in the coronal and transverse planes are limited and can be considered as negligible. Although significant research has been performed, the pelviperineal physiology and the anatomic basis of pelvic floor diseases remain unclear, as mentioned in [42] and [32]. Some works attempted to analyze the pelvic dynamics, such as [8], where the authors propose to measure the organ descent with the dynamic MRI. The study concerned several patients of different age, aiming at evaluating the effect of aging. The measurements were done manually, which limits the reproducibility of the analysis. An image-analysis based study could bring a quantitative characterization of the pelvic organ dynamics. As it would be automatic, it could be applied to a wide number of cases. In [37], a global characterization of the deformations of the pelvic organs has been proposed. It uses shape descriptors to measure shape variations of the pelvic organs, but it does not track the local dynamics of organ specific landmarks. In this paper we present an organ dynamics characterization methodology based on the current representation of the curves and the diffeomorphic mapping, by performing a statistical group analysis. The approach allows to analyze the organ behavior locally, and to compare different organ behaviors from different MRI sequences. Its main advantage is that it takes into account the large organ deformations that are observed along a dynamic MRI. Starting from the available sequences, the methodology is decomposed into three stages : Firstly, the diffeomorphic matching of the sequences is performed for each organ against a template shape. Secondly, deformation features are computed on each organ points. Finally, the estimated features are used for the quantitative assessment of the pelvic dynamics. This is done through a statistical analysis, where the principal deformation modes of the organs are calculated. Then, organ parcellations are performed according to the feature variations.

In addition to the pathophysiology comprehension purpose, this methodology will take place in the patient-specific pelvic dynamics modelling framework proposed in [5], which aims at simulating numerically the behavior of the pelvic organs. The solution could be integrated into the preoperative planning, in order to assist the surgical handling. In this sense, the dynamic MRI characterization would serve as ground truth for the modelling validation, and for a prospective correction.

We detail in section 3 the proposed approach for the organ dynamics characterization. Some results are presented and discussed in section 4, where the pathology detection capability of the computed features is analyzed through an inter-patient analysis, in addition to a local organ analysis. Section 5 concludes the paper.

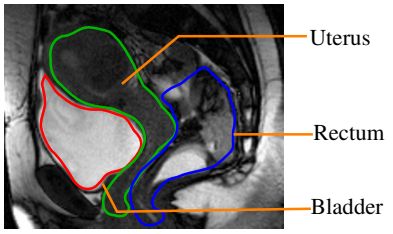

(a) The main pelvic organs.

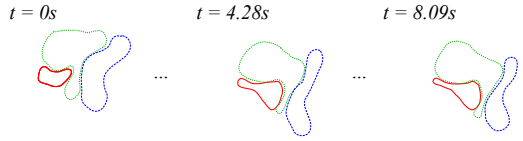

(b) A segmented MRI sequence.

Fig. 1 The main pelvic organs (bladder, uterus-vagina, rectum) on the median sagittal plane.

2 Related Work

Computational anatomy yields a large field of temporal evolution studies of free-form and deformable objects. The spatio-temporal statistical analysis of the anatomical structures is a key step for the physiological comprehension and interpretation of the phenomena involved. For instance classification is achievable on large datasets aiming at pathology detection. The statistical analysis may be used also for the segmentation [36]. A shape variation model of the structure is computed from available samples, this prior-shape will be used as a criterion for the segmentation.

Classical approaches of anatomical structures analysis handle sets of anatomical landmarks. We cite the studiy of [31], where eigen-shapes are computed starting from anatomical structures having the same amount of landmarks. In [24],

the authors proposed a procrustes analysis. They compare two shapes a and b through their homologous points, by deforming the points of b so that they get as close as possible to the points of a, thanks to translations, rotations, and scalings. Among the drawbacks of this method is the fact that it is based only on landmarks, which limits its applicability on data without anatomical references. Moreover, the method uses a least-square criterion for the optimization, which implies that a local variation of a landmark will have a global influence on the location of all the landmarks.

We find in the litterature diverse methods of statistical shape analysis [12]. The diversity of these methods particularly resides in the type of the studied data. In [1] the authors performed a morphological analysis of cerebral structures based on the voxel intensity of MRI data. [21] shows the use of a skeleton-based representation of corpus callosum shapes. The approaches also differ in terms of the mathematical tools used. For example, a machine learning based method for the statistical analysis was proposed in [41], where a linear discriminant analysis classifier is used for the human brain analysis. However, the dataset size used for the learning step is decisive for the determination of the approach feasibility. Furthermore, [9] presents a model based method. The model describes the distribution of the shape variations, it relies on a mixture of Gaussian kernels in each shape point. Such an approach allows a representation of the non-linear variations of the shape, even if it necessitates a rigorous parameterization in order to obtain significant results.

In fact, both the choice of the shape representation and the method used depend crucially on the application and the nature of the data.

When handling a deformable anatomical structure without fixed landmarks and having anisotropic deformation, the analysis requires to find a correspondence between the structure points. An elastic mapping method is used in order to estimate the structure deformation.

Recently, the diffeomorphic mapping method has presented some interesting properties. This non-linear registration is based on a smooth and invertible deformation function which maps a shape to another. The problem was initially addressed by [13]. Since then, several variants have been proposed according to the nature of the data (points, curves, surfaces). Then, the statistical analysis assesses the evolutions of the anatomical structure points. Other approaches advocate to perform statistics on the deformations rather than the points, as in [39] and [15].

The methodology proposed in this paper relies on the diffeomorphic mapping in order to measure the pelvic organ behaviors. To our knowledge this is the first characterization of the pelvic organ dynamics with a shape statistical analysis.

Among the studies related to the pelvic cavity, we refer to the works of [22], aiming at the achievement of a simulator of hysteroscopy. The authors studied the morphological differences of a synthetic uterus. It deals with a geometric model of the uterus which is deformed under different strain conditions. Another study *somewhat* linked to the pelvic dynamics was proposed by [40], where a statistical analysis relative to the detection of the pelvic disorders is performed through a questionnaire on 800 patients. The survey allowed to generate a predictive model of the uterine prolapse risks.

3 Sequence Characterization Methodology

Within the context of the pelvic organ dynamics analysis, the lack of anatomical references and the large morphological variability of the organs constrain our approach.

Figure 2 summarizes the shapes of the bladder contours for each patient at different times of the bladder dynamics. Each line represents the bladder contours of one patient, and each column represents different patient contours at a given time of the dynamics. A mere visual observation reveals that there is a large shape variability of the pelvic organs as they are soft-tissue organs. This is the main reason for our focus on the dynamics of the organ and its deformation evolution during a strain. The evolution is assessed by comparing the organ to its shape at the rest state ($t = 0$).

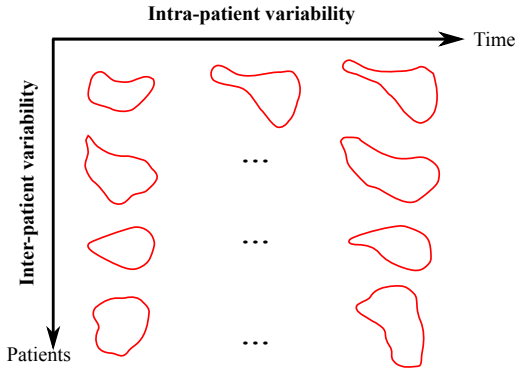

Fig. 2 Illustration of the morphological variability of the bladder.

As depicted in figure 3, the proposed approach for the characterization takes as input the organ contours. It relies on three steps : The organ mapping in order to find a correspondence between the points of the organ contours at different times of a sequence. Then, features are extracted from the mapped points, they describe the evolution of the organ contour. Finally, a statistical analysis is performed to quantify the dynamics of the organs, and to highlight characteristic behaviors.

In the following sections, we will detail each step of the characterization flowchart depicted in figure 3.

Fig. 3 Pelvic organ dynamics characterization pipeline.

3.1 Notations

Let be $\mathscr{S}$, the set of the contour sequences for a given organ *org* :

$$\mathscr{S}_{(org)} = \{S_1, S_2, \ldots, S_i, \ldots\} \tag{1}$$

Where $i = 1, \ldots, N_{\mathscr{S}}$, $N_{\mathscr{S}}$ is the cardinal number of the set $\mathscr{S}$. It represents the number of sequences.
org $\in$ { bladder, uterus-vagina, rectum }.
A temporal sequence S_i composed of N_{S_i} ordered contours is:

$$S_i = (S_i^0, S_i^1, \ldots, S_i^j, \ldots) \tag{2}$$

For this purpose, a pre-processing step has been applied to obtain an ordered contour curve S_i^j, where each point $s_i^j(t) = (x(t), y(t))$.
Then, $\mathscr{S}^0$ is the set of the *org* shapes at $t = 0$:

$$\mathscr{S}^0_{(org)} = \{S_1^0, S_2^0, \ldots, S_i^0, \ldots\} \tag{3}$$

Where $i = 1, \ldots, N_{\mathscr{S}^0}$, with $N_{\mathscr{S}^0} = N_{\mathscr{S}}$.

3.2 Organ Mapping

The goal of the organ mapping is to define a coordinate system common to all the organ contours. Some simple solutions can be considered like using the curvilinear coordinates, or using the Bookstein coordinates [6]. But the unavailability of landmarks and the large morphological variability in our case make those solutions poorly efficient.
To address this issue we perform a non-rigid registration which takes into account the morphological variability. The geometric registration implies to find the optimal transformation of a geometric structure to another one. The constraints imposed by the nature of the data led us to look at non-rigid registration methods. Reviews of medical image registration, and the non-rigid registration are proposed respectively in [33], and [11]. Among the registration techniques, Large Deformation Diffeomorphic Metric Mapping (LDDMM) algorithms have recently received a great attention. They provide diffeomorphic maps (one-to-one), reversible smooth transformations that preserve topology. The interest of the choice of this method resides in the fact that it can map very irregular deformations. The LDDMM allows large deformations and constrains their regularity. Its mathematical formulation includes a data-fidelity term, and a regularity term not only on the final solution, but also on the evolution of the deformation.

3.2.1 Large Deformation Diffeomorphic Metric Mapping

The LDDMM is a non-linear registration method. It defines a mapping function ϕ, which is a diffeomorphism since it is invertible and differentiable. One of the benefits of the method relies in its ability to map very irregular deformations, resulting on a smooth displacement field, regular, and without intersections. The LDDMM can be applied to different geometrical structures, such as surfaces, curves, sparse points, or landmarks. The method has been used, among others, for the inter-subject registration of cortical surfaces [2], the analysis of the temporal evolution of the skull [14], or the estimation of an anatomical atlas [4].
We will focus in this paper on the LDDMM applied on curves, as we handle organ contours, which can be considered as sets of ordered points. The curve LDDMM method is detailed in [20].

3.2.1.1 Curve Representation Based on "Currents" : The heart of the method is based on the representation of the curve, also known as the current representation. It embeds both location and tangential information at each point of the curve.
For a curve C, a parameterization γ_C is defined as :

$$\begin{array}{rccc} \gamma_C : & [0,1] & \longrightarrow & \mathbb{R}^d \\ & s & \longmapsto & \gamma_C(s) \end{array} \tag{4}$$

$\gamma_C{}'(s)$ is the corresponding tangent. The following formula represents μ_C the current representation of C under a vector field w :

$$\langle \mu_C | w \rangle = \int_0^1 \gamma_C{}'(s).w(\gamma_C(s))ds. \tag{5}$$

The advantage of this representation is that the matching method is curve parameterization independent, *i.e.* we can have two curves with two different point sizes and sampling, besides we have two complementary informations (location, tangent).
Then, a curve metric is defined thanks to this representation, on the dual space W^* of a Hilbert space W with a kernel k_w as follows :

$$\|\mu_C\|^2_{W^*} = \int_0^1 \int_0^1 [\, k_w(\gamma_C(s), \gamma_C(r))\ \gamma'_C(s)\,] \,.\, \gamma'_C(r)\, ds\, dr. \tag{6}$$

Also, a distance between two curves C and C' can be computed as follows :

$$\|\mu_C - \mu_{C'}\|^2_{W^*} = \|\mu_C\|^2_{W^*} + \|\mu_{C'}\|^2_{W^*} - 2\int_0^1\int_0^1 [k_w(\gamma_C(s),\gamma_{C'}(r))\ \gamma'_C(s)]\,.\,\gamma_{C'}{}'(r)\,ds\,dr. \quad (7)$$

3.2.1.2 Diffeomorphic Mapping : Regarding the mapping of two shapes A source and B target, the LDDMM principle relies on modelling the mapping ϕ by a dynamic flow of diffeomorphisms v_t, enabling the deformation of B to A.
To obtain the mapping ϕ_t^v, we have to compute the time-dependent vector field v_t. The two terms are linked by the equation

$$\frac{\delta\phi_t^v}{\delta t} = v_t(\phi_t^v), \quad (8)$$

with $\phi_0^v(B) = B$, and $\phi_1^v(B) = A$. v_t belongs to Hilbert space V with a kernel k_V, this property ensures that the final solution is a diffeomorphism.
So the mapping ϕ provides not only the correspondence between A and B, but also the optimal flow between the two shapes, which represents the geodesic path from B to A. An illustration of this path is showed in figure 4, where the successive deformations of the target (ϕ_t.B) are highlighted, until they reach the source A.
The mapping problem is formulated by finding v_t that minimizes :

$$J_{B,A}((v_t)_{t\in[0,1]}) = \gamma\int_0^1 \|v_t\|^2_{V^*}dt + E(\phi_1^v.B,A). \quad (9)$$

The first term is a regularization term that controls the smoothness of the diffeomorphism, the second term is a data attachment term which quantifies the matching error between the mapped target points $\mu_{\phi_1^v(B)}$ and the source points μ_A.
The deformation map (ϕ_1^v) has to be determined. This is done thanks to an approximation of the correspondence between the two curves, by optimizing formula (9), where the minimization concerns an energy E which measures the similarity between the deformed B and A.
The data-fidelity term is computed by using the tangential current representation of the curves, in the dual space of a Hilbert space W with a kernel k_w as follows :

$$E(\phi_1^v.B,A) = \|\mu_{\phi_1^v(B)} - \mu_A\|^2_{W^*}. \quad (10)$$

Typically, the minimization of (9) is done with the conjugate gradient method. We used the implementation presented in [20].

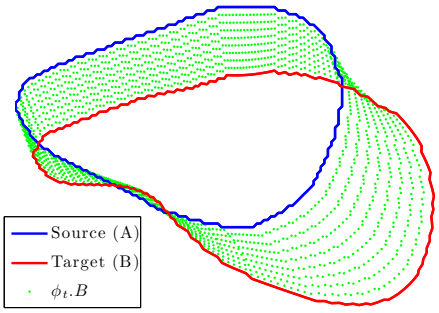

Fig. 4 An illustrated example of a two shapes (blue, red) matching, the dotted shapes are the intermediate deformed shapes according to ϕ.

3.2.2 The Proposed Mapping

For each organ, we define a spatial reference which is common to all the studied sequences, so that we can track the contour points of the pelvic organs.
Our approach is based on the LDDMM and the tangential current representation. First, a *template shape* is computed in order to unify the parameterization of all the sequences. The template is selected from the available data, it should minimize a metric based on the shape currents. Then regarding the template shape an *inter-sequence mapping* is performed with the LDDMM. It provides a common spatial reference for all the shapes at the rest state allowing to track the points on different sequences.
At last, we use the *intra-sequence* mapping between the current organ shape and the shape estimated from the inter-sequence mapping. It produces the deformation field of the organ points along a sequence of frames.
We detail in the following paragraphs the template computation and the mappings implemented.

3.2.2.1 Template Computation This step determines the reference on which will be mapped the initial sequence contours.
Many works attempted to perform this task ([26], [34]), by computing a template based on registrations, which ensure an unbiased estimation of the template. In our case, we consider that we have a sufficient number of organ shapes, so we can determine a template shape from this set.
We define a template shape T as a shape which will be the reference for the inter-sequence mapping. In order to have an anatomically consistent template, it should be a mean shape which belongs to the initial shapes set $\mathscr{S}^0$, rather than an approximation with a statistical mean. This led us to look at the Fréchet mean. For a set $M = \{x_1, \ldots, x_i, \ldots, x_n\}$, the Fréchet mean aims at finding an element $p \in M$, by mini-

mizing the distance d, weighted by the coefficients w_i.

$$m = \underset{p \in M}{\arg\min} \sum_{i=1}^{n} w_i d^2(p, x_i) \tag{11}$$

So the template T should minimize the distance between the shapes S_i^0. We use the current based representation of the contours described previously, and the metric defined in (7) to compare the contours. The metric of currents depends on the kernel k_w, which can be considered as a smoothing parameter of the shape. Taking a small kernel will take into account all the shape little variations, and a taking a big one will make it insensitive to these variations which may be assimilated to segmentation errors. So the standard-deviation of k_w has been set with respect to the mean size of the organ translations.
Therefore, we propose the following formulation for the template estimation :

$$T = \underset{T \in \mathscr{S}^0}{\operatorname{argmin}} \sum_{i=1}^{N_{\mathscr{S}}} \frac{1}{\sigma^2_{S_i^0}} \| \mu_T - \mu_{S_i^0} \|^2_{W^*} \tag{12}$$

$\sigma_{S_i^0}$ is the standard deviation of the shape S_i^0 relative to the set $\mathscr{S}^0$:

$$\sigma^2_{S_i^0} = \frac{1}{N_{\mathscr{S}} - 1} \sum_{j=1}^{N_{\mathscr{S}}} \| \mu_{S_i^0} - \mu_{S_j^0} \|^2_{W^*} \tag{13}$$

Using the standard-deviation coefficients as weights allows to give less importance to extreme contour locations and variations, which are generally considered as outliers. Also, a rigid registration is performed before the template computation, by the Gaussian mixture rigid registration proposed by [25]. So all the $\mathscr{S}^0$ shapes have been aligned in order to ensure the invariance to the translation and the rotation.

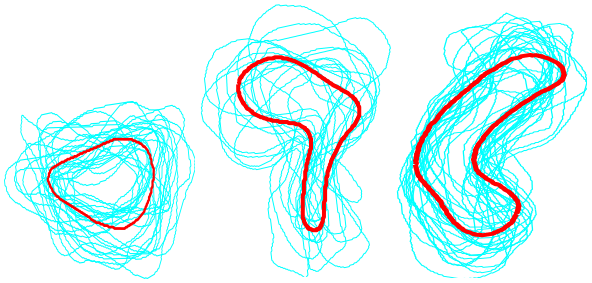

(a) Bladder (b) Uterus (c) Rectum

Fig. 5 Results of the Template Shape Computation. In red the templates selected.

3.2.2.2 Inter-Sequence Mapping For a given organ, the inter-sequence mapping aims at determining a common contour parameterization. It involves the curve matching between the template shape (T) and the organ shapes at rest states from different sequences (S_i^0), by using the LDDMM formulation in equation (9).
For an initial shape S_i^0 and the template T, the inter-sequence mapping function (ϕ_1) is defined as follows :

$$\phi_1(S_i^0, T) = {S'}_i^0. \tag{14}$$

Where ${S'}_i^0$ is the mapped shape to the template.

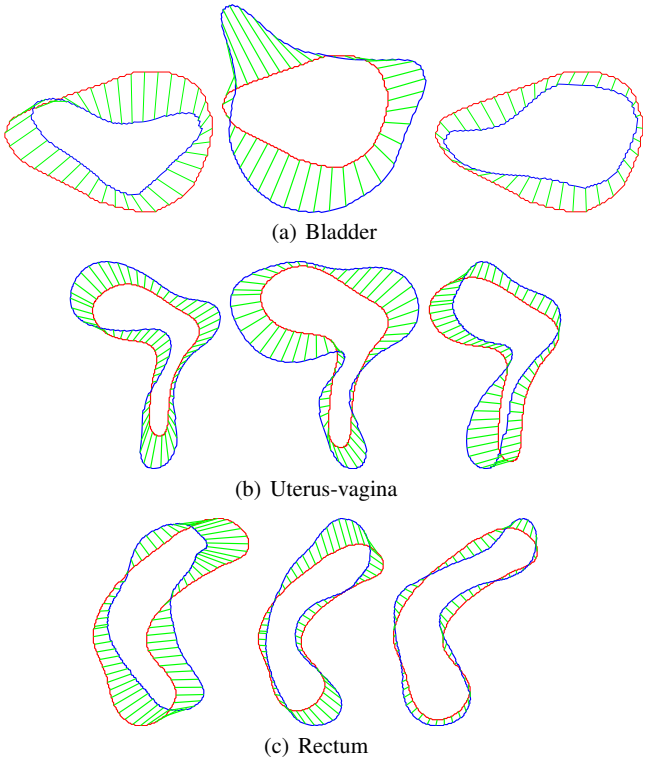

(a) Bladder

(b) Uterus-vagina

(c) Rectum

Fig. 6 Some results of the inter-sequence matching between different initial shapes (blue) and the associated templates (red).

3.2.2.3 Intra-Sequence Mapping Thanks to the inter-sequence matching, all the contours of a given organ type (bladder, uterus or rectum) at rest share a common parameterization. So each organ contour point is clearly identified. The intra-sequence analysis aims at tracking each contour point over time. This is done by matching the organ points at the j^{th} frame towards the corresponding points of the initial organ shape. This matching is obtained with a composition of consecutive matching $(k, k+1)$, starting from the initial contour ${S'}_i^0$ to the contour ${S'}_i^j$ (figure 7).
For a shape S_i^j, the intra-sequence mapping function (ϕ_2) is defined as follows :

$$\phi_2(S_i^j) = \phi({S'}_i^0, S_i^1) \circ .. \circ \phi(S_i^k, S_i^{k+1}) \circ .. \circ \phi({S'}_i^{j-1}, S_i^j) \tag{15}$$

This technique involves estimating a large deformation with a composition of consecutive deformations and consequently smaller ones. It avoids the inaccuracies due to very large deformations that occur between the first and the last frames of the sequence.

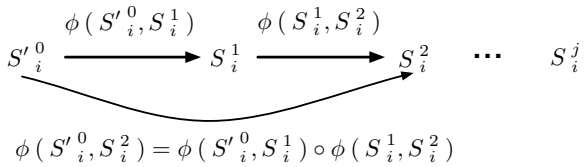

Fig. 7 Diagram of the LDDMM matching on a contour sequence.

3.3 Feature Extraction

Once the organ contours are mapped, we have a correspondence between the organ points. So the mapping **M**, for a given organ of a sequence S_i :

$$\mathbf{M}_i(\text{organ}) = \begin{pmatrix} p^{1}_{1} & . & p^{N_s}_{1} \\ . & p^{j}_{k} & . \\ p^{1}_{N_c} & . & p^{N_s}_{N_c} \end{pmatrix}. \quad (16)$$

Where $p^{j}_{k} = (x_k, y_k)^j$ are the coordinates of the k^{th} contour point, of the j^{th} frame in the sequence. N_s and N_c are the number of frames and the number of contour points respectively.

In addition, the LDDMM provides deformation function ϕ, which represents smooth deformation paths between each consecutive contours, providing intermediates contours.

Some works analyze deformations rather than handling point correspondences, like in [15], where the brain variability is assessed by performing statistics on the deformations. The deformation momentum is a global deformation feature that can be directly extracted from the LDDMM [39]. It quantifies the amount of the deformation between two organ contours. This feature is equivalent to the global shape descriptors proposed in [37]. It will not be used in this study, as the aim of the feature analysis is the local characterization of the organ behaviors.

Since we want to evaluate the organ tissue behaviors and to estimate some biomechanical measurements on the organs, the proposed features describe the dynamics of the contour points. In addition , as mentioned in introduction, that could bring some clues about the pelvic organ dynamics modelling.

The features used are detailed in the following subsections. They are complementary, as they describe distinct properties, and express the empirical descriptions of the pelvic dynamics done by the clinicians.

3.3.1 Displacement Field Magnitude

As a result from the LDDMM mapping, the displacement vectors for each subject are obtained. These displacement vector fields describe the effects of the deformation of the organ, compared to the rest-state of this organ. The displacement magnitude D^{j}_{k} of a point $p^{j}_{k} = (x^{j}_{k}, y^{j}_{k})$ at the j^{th} frame compared to its initial state ($t = 0$) is defined as the cumulative distance of the m intermediate points between the rest state and the j^{th} frame, with $m < j$:

$$D^{j}_{k} = \sqrt{\sum_{m=1}^{j-1} [(x^{m+1}_{k} - x^{m}_{k})^2 + (y^{m+1}_{k} - y^{m}_{k})^2]}. \quad (17)$$

3.3.2 Tensor Based Deformation Features

Among the methods used for the anatomical structure analysis, the tensor-based morphometry method has been used for the brain analysis in studies of Alzheimers disease [18], and HIV/AIDS ([7],[30]). The principle of the method is to calculate the displacement gradient, also known as the Jacobian matrix, based on the image voxels typically. Let us consider a 2D point $p = (x, y)$ of a shape and its transformation $U = (U_x, U_y)$, the jacobian matrix is

$$J(p) = \begin{pmatrix} \partial U_x/\partial x, & \partial U_x/\partial y \\ \\ \partial U_y/\partial x, & \partial U_y/\partial y \end{pmatrix}. \quad (18)$$

The jacobian determinant is used also as a criterion for the registration regularization in [35], it constrains the deformation during the transformation optimization.

We have been interested in deformation features in the mechanics sense. In other words, we looked at features which characterize the biomechanical properties of the organ tissues. Usually, these features are the elongation and the angular distortion [29]. They are computed at each organ contour point, as we consider the contour as an ordered set of points.

The mechanical measurements are defined on small deformations, while the pelvic organs undergo large deformations. So we use the intermediate shapes computed with the diffeomorphic function ϕ, thanks to the LDDMM. As it provides smooth shape deformation, it will ensure consistent results.

3.3.2.1 The Elongation Feature This deformation descriptor is also called the Green-Lagrange deformation. It measures the level of the spacing in the neighborhood of a point.

As showed on figure 8, p_k^j and p_{k+1}^j are two consecutive points of the initial shape of the j^{th} frame. p_k^{j+1} and p_{k+1}^{j+1} are their homologous points on the $(j+1)^{\text{th}}$ frame, according to a deformation vector $\overrightarrow{U}$. The elongation E_k^j is the ratio between the pair $(p_k^j,\ p_{k+1}^j)$ noted by the vector $d\overrightarrow{X}$, and $(p_k^{j+1},\ p_{k+1}^{j+1})$ noted by the vector $d\overrightarrow{x}$. It is calculated as follows

$$E_k^j = \frac{\|d\overrightarrow{x}\|^2 - \|d\overrightarrow{X}\|^2}{2.\|d\overrightarrow{X}\|^2}. \tag{19}$$

$|E| = 0$ means that no deformation has occurred, and when $|E| > 0$, the neighborhood of the point has expanded. Otherwise, the neighborhood has shrunk.

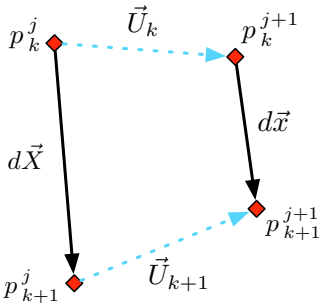

Fig. 8 Illustration of the elongation at the neighborhood of p_k^j and p_{k+1}^j, caused by the deformation vector field U.

3.3.2.2 The Angular Distortion Feature It is the resulting angle of the deformation of three close points. Let's have three consecutive points p_{k-1}^j,p_k^j,p_{k+1}^j (figure 9), the angular distortion Θ is the difference between the two angles $\theta = \widehat{p_{k-1}^j\, p_k^j\, p_{k+1}^j}$ and $\theta' = \widehat{p_{k-1}^{j+1}\, p_k^{j+1}\, p_{k+1}^{j+1}}$:

$$\Theta_k^j = \frac{d\overrightarrow{x_1} \cdot d\overrightarrow{x_2} - d\overrightarrow{X_1} \cdot d\overrightarrow{X_2}}{\|d\overrightarrow{X_1}\| \|d\overrightarrow{X_2}\|} \tag{20}$$

Intuitively, a null angle means that there is no local deformation. Otherwise, it is a measure of the aperture change.

3.4 Feature Analysis

In the analysis of the extracted features, we study each organ separately. The analysis aims at characterizing the pelvic organ behaviors, but also validating the consistency of the chosen features. The proposed analysis methods are described in the sections below.

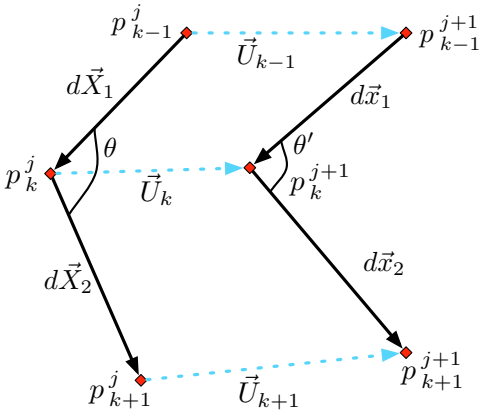

Fig. 9 Illustration of the angular distortion at the neighborhood of p_{k-1}^j,p_k^j, and p_{k+1}^j, caused by the deformation vector field U.

3.4.1 Feature Relevance Assessment

To compare the performance of the computed features, the feature relevance is assessed. By relevance, we mean the pathology detection capability. More precisely: we have sequences of several patients, in addition, we have the clinical diagnosis (healthy / pathological) of each pelvic organ. A group analysis on all the sequences is performed for a given organ, according to the different deformation features presented above. It allows to assess qualitatively the feature capability to separate the pathological cases from the healthy ones.

We opted for exploratory data methods for the assessment, rather than predictive methods such as the classification. This choice is motivated by the fact that we have a limited number of sequences. We consider that a classification rate computed from a small dataset may not be significant enough. So the qualitative evaluation is done with a projection of the data on a reduced dimension space.

Thus, for a given patient, the dynamics of an organ composed of N_c points is summarized by the vector

$$F_i(\text{organ}) = (\, f_1\, , \ldots ,\, f_k\, , \ldots ,\, f_{N_c}\,), \tag{21}$$

where each element is the feature at a contour point, *i.e.* : $f_k \in \{D_k, E_k, \Theta_k\}$. Thus, for a set of $N_{\mathscr{S}}$ patients, we have

$$\mathscr{F}(\text{organ}) = \begin{pmatrix} F_{\,1}\,(\text{organ}) \\ \cdot \\ F_{\,i}\,(\text{organ}) \\ \cdot \\ F_{\,N_{\mathscr{S}}}\,(\text{organ}) \end{pmatrix} \downarrow \textit{patient}. \tag{22}$$

$\mathscr{F}$ is a $N_{\mathscr{S}} \times N_c$ matrix.

We perform a dimension reduction on the feature space of the P patients. For this purpose, we use the *Multidimensional scaling* (MDS) method [10]. This method is often used in information visualization context for exploring similarities or dissimilarities within data. It takes as input a similarity matrix Δ between the data items, and provides the

item coordinates in another space with a different dimension, thanks to a minimization of a loss function called "*stress*". Typically, the problem consists in finding N components c which minimizes the stress :

$$\min_{c_1,\dots,c_N} \sum_{i<j} (\|c_i - c_j\| - \delta_{i,j})^2, \tag{23}$$

where $\delta_{i,j}$ is an element of the similarity matrix Δ. In our case, the similarity matrix is computed on the $N_{\mathscr{S}}$ patients. We have fixed the representation dimension value at 2, so that we can visualize the patient organs with their diagnoses on a 2D plan as depicted in figure 10

3.4.2 Organ Behavior Characterization

In order to extract the characteristic behaviors, the statistical differences between the available sequences are computed. This requires the estimation of a mean behavior of the organ contour points, for pathological and healthy cases. The organ behavior is described by the features F computed previously on all the sequences. Then, we carry out a principal component analysis (PCA) for the extraction of the main deformation modes on two groups (healthy and pathological). The PCA's main objective is to find a projection matrix that maximizes the variance-covariance matrix. In our case, the matrix $\mathscr{F}$ in equation (22) is divided into two sub-matrices : $\mathscr{F}_1$,$\mathscr{F}_2$ for the healthy cases and the pathological cases, respectively. The PCA computes the eigenvalues and the eigenvectors associated to the matrix $\mathscr{F}_i^{\mathbf{t}}\,\mathscr{F}_i$. The largest eigenvalues associated with the eigenvectors represent the principal modes of deformation. This analysis enables to take into account the global correlations of all point motions, and highlights the main trends of deformation from the available sequences, for the pathological and healthy cases.

3.4.3 Organ Local Analysis

With the deformation features, it is possible to track the dynamics of each organ point on each sequence frame. The purpose of the local analysis of the organ contours is to gather their points, according to the similarity between the computed features. It seems obvious to use a method of unsupervised clustering. The clustering determines groups [16] and each data item is assigned to one of these groups. The problem common to the majority of the clustering methods is the determination of the number of the clusters. A solution proposed in [3] relies on a dynamic clustering. It uses thresholds on intra-class homogeneity criteria. So classes are merged or split according to these thresholds. Unfortunately, there is no automatic method for the determination of these thresholds.
Among the many existing clustering methods, we opted for the *Affinity propagation* method proposed in [19]. Its main advantage lies in the automatic determination of the number of clusters when this latter is not known in advance. The method is fully explained in [19]. Briefly, having N items to be clustered, the method takes as inputs the similarity matrix $\mathfrak{M}$ between the N items. The number of clusters is initialized to N, in other terms, all items are *a priori* selected as exemplars. Two kinds of values are computed, namely the "*responsibility*" and the "*availability*". The responsibility $r(i,k)$ is transmitted from item i to item k, it reflects how well-suited k is to serve as the exemplar for i. The availability $a(i,k)$, is transmitted from candidate exemplar item k to item i, it reflects the accumulated evidence for choosing k as the exemplar of i. Then, the responsibility and availability values are updated on each item, at every iteration, as follows :

$$r(i,k) \leftarrow \mathfrak{m}(i,k) - \max_{k' \neq k} \{a(i,k') + \mathfrak{m}(i,k')\}, \tag{24}$$

$$a(i,k) \leftarrow \min\{0, r(k,k) + \sum_{i' \notin \{i,k\}} \max\{0, r(i',k)\}\}. \tag{25}$$

This allows to group the items after a given number of iterations, where the number of classes decreases from N to n.
In our case, the affinity propagation is used to find a parcellation related to the dynamics of the deformations, for a given organ. The features of the used dynamics are the ones defined in section 3.3. The similarity matrix $\mathfrak{M}$ is built from these features. It contains the distance between the different features of the organ N points at different times,

$$\mathfrak{M} = \{\mathfrak{m}(i,j) = d_{\text{euclidean}}(v(i), v(j)), 1 \leq i,j \leq N\}. \tag{26}$$

Each element $\mathfrak{m}(i,j)$ represents the Euclidean distance between i^{th} and j^{th} temporal feature vector v, of the i^{th} and j^{th} contour points.

4 Results and Discussion

We present in this section the main results of the methodology described in section 3. The results are gathered in two parts : the inter-subject analysis on the whole available data, and the local organ analysis, for each individual organ.

4.1 Data

In this study, we used a dataset of 30 segmented sequences, where each sequence contains $m = 12$ frames (1 frame per second). The dynamic MRI sequences are $2D+t$ MRI strain image acquisitions in DICOM format, performed with 1.5T PHILIPS *Gyroscan* on the sagittal plane, by using an ultrafast T2-weighted pulse sequence ($tr = 3.6ms$, $te = 1.8ms$, $thickness = 10mm$, FOV $= 24cm$).
In addition, we have the clinical diagnosis related to each organ of the segmented pelvic MRI.

Table 1 lists the number of the pathological organs studied and the healthy ones. One should notice that 10 patients among the 30 underwent a hysterectomy, so only 20 uteri were available.

Table 1 Available Data

	Pathological	Healthy
Bladder	16	14
Uterus	8	12
Rectum	13	17

4.2 Inter-Subject Analysis

4.2.1 Feature Relevance

The purpose of the inter-patient analysis is to assess the ability of the deformation estimators towards the discrimination between MRI sequences. We have applied the MDS analysis on all the features of all the sequences, for each organ. The feature space dimension has been reduced to 2. The quality of the dimension reduction is assessed by the final value of the MDS stress criterion. The stress values of each reduction performed in our case belong to $[10^{-6}, 10^{-4}]$. These values validate the soundness of the reduction, as a consistent dimension reduction generally leads to a stress value below 0.1.

The MDS results are depicted in a 2D plan in figure 10, where each point represents one patient. In most cases, we observe an evident separation between pathological organs (red triangles), and healthy ones (green squares). A better separation is seen on the bladder than on the uterus and the rectum. This makes it possible to say that the features seem to be less discriminating in detecting rectoceles, where the disease is mainly characterized by the descent of the organ. This result is explained by the difficulty of rectum segmentation, as the rectum represents the continuity between and the intestine and the anus, which makes difficult the delineation of the rectum upper limits, and introduces a large variability. The inter-feature comparison shows that the angular distortion provides a weak separation between the two groups. Then, the distortion feature is less efficient for the pathology detection. This may be explained by the approximation errors made during the computation of the angles. Nevertheless, we can assert that the deformation features calculated are relevant criteria aiming at distinguishing in between pelvic organs those with disease and the healthy ones.

4.2.2 Deformation Modes

Another aspect of the group analysis is to calculate the deformation modes. Starting from the available data, this analysis yields the principal kinds of deformations of an organ. We have calculated the deformation modes by using the PCA, as described in section 3.4.2. In fact, for each feature of the organs, a mode specific to the pathological cases is computed, as well as a healthy case mode. We used as features the two components of displacement field, and the deformation features (elongation, distortion). The results are summarized on figure 11.

On the deformation modes of the whole organs, we see stronger magnitudes of the displacement, the elongation, and the distortion in the pathological mode compared to the healthy mode.

The bladder is characterized by a vertical movement in its cranial (upper) part, which is due to the response of the diaphragm strain force. The ventral part of the bladder moves slightly. We explain this observation by the fact that this part is in contact with the pubic symphysis, which is a rigid osseous structure. We also note the highlighting of a significant elongation in the caudal part of the bladder.

Concerning the uterus-vagina, the healthy mode shows a vertical movement from top to bottom of the cranial part of the uterus, while ventral part of the uterus and the vagina undergo lateral displacements. The justification of this observation is that the vertical movement corresponds to the response to the diaphragm strain force, whereas the lateral displacements are caused by the dynamics of the bladder. Also, according to the elongation and the distortion based modes, the uterus undergoes less deformations than the vagina. This observation confirms that the elasticity of the vagina is larger than the uterus elasticity.

The rectum displacements shows lateral displacements, even if the anus is going vertically. The anterior wall of the rectum seems to undergo more elongation and distortion than the posterior part.

On the whole, clinical knowledge and observation corroborate the main modes pointed out by the analysis. Moreover, we observe an anisotropy on some organ regions which undergo deformations. This non-homogeneity will be analyzed in the following section.

4.3 Organ Parcellation

The local analysis of an organ, also called "*organ parcellation*", aims at grouping the organ contour points which have a high correlation during the organ dynamics. The grouping is based on the evolution of the dynamics features. One should notice that the similarity matrix is different from the one used in the feature evaluation. Indeed, for the organ parcellation, each organ has its own similarity matrix made of the comparison between the feature evolutions. Some results are showed in figure 12. From the bladder parcellation results, two to three separate sectors (blue, red, green) are distinguished. In figure 12(a), the blue and green sectors corre-

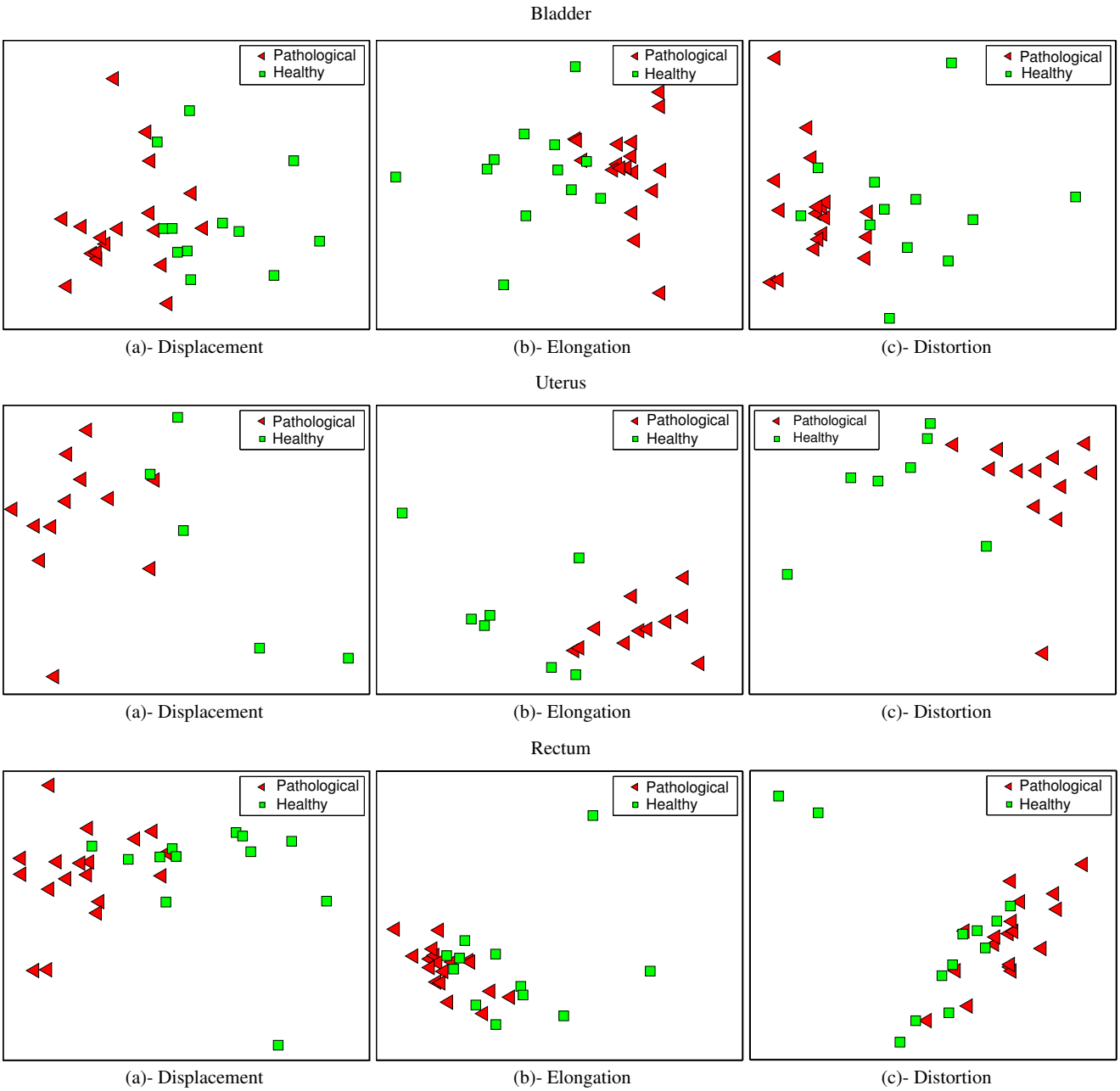

Fig. 10 Feature relevance assessment through the MDS analysis on the three features (displacement, elongation, distortion), applied on the three pelvic organs.

spond to the upper edge of the bladder which undergoes less deformation than the lower edge of the bladder delimited by the red contour. This result is anatomically interesting as the delimited sectors involve two anatomical references. Indeed, the point undergoing the maximal deformation corresponds to an anatomical landmark called the bladder neck, the blue parcel includes the attachment point of the bladder to the urachus, while the red parcel includes the bladder neck.

Two to three sectors characterize the uterus (figure 12(b)), they separate the uterus from the vagina. In addition, the deformation magnitude of the sectors related to the vagina are larger than their uterus counterparts, corroborating the fact that the uterus is more rigid than the vagina.

Concerning the rectum (figure 12(c)), we observe a separation between the rectal bulb and the anal canal (in red) as they have different behaviors and different rheological properties. Also, the posterior part of the rectum undergo less deformation than the anterior part which is linked to the dynamics of the other organs. Overall, besides automatically highlighting the non-homogeneous deformations of pelvic

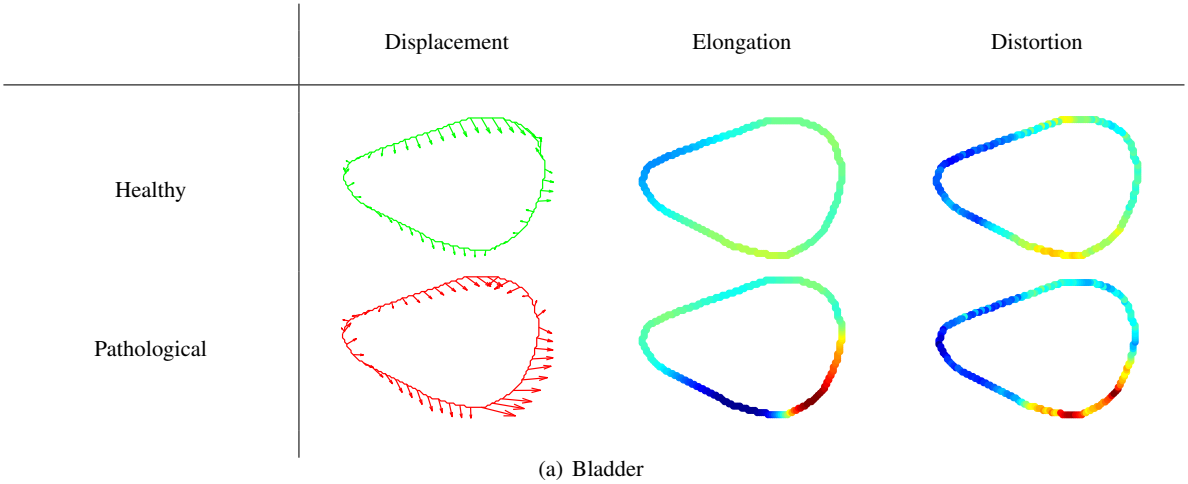

(a) Bladder

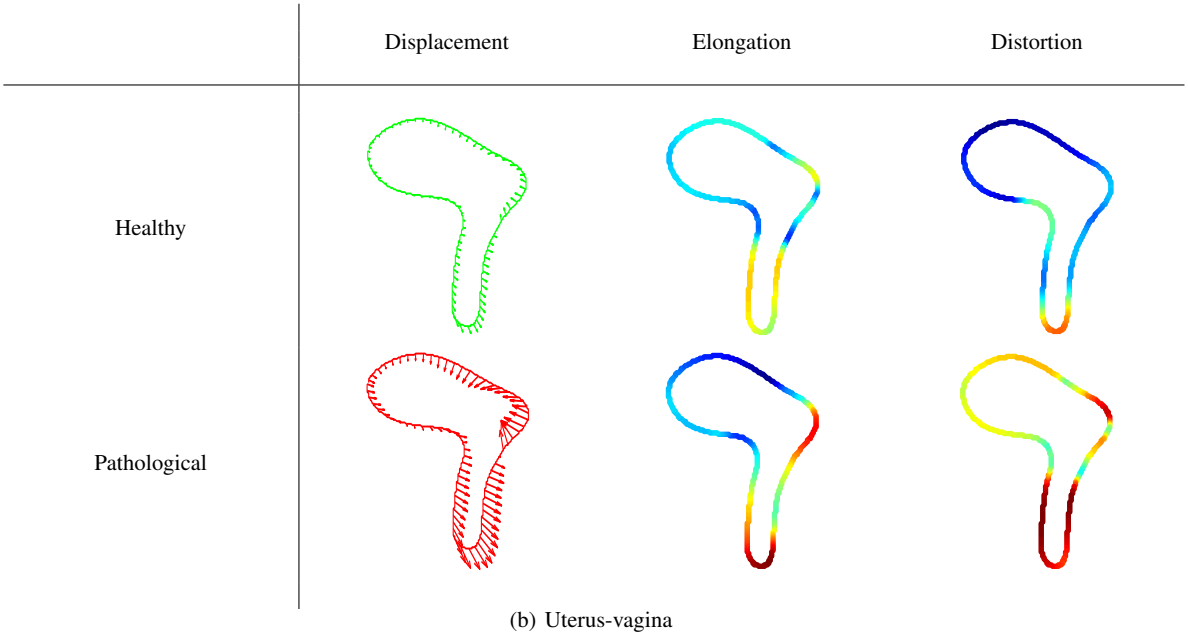

(b) Uterus-vagina

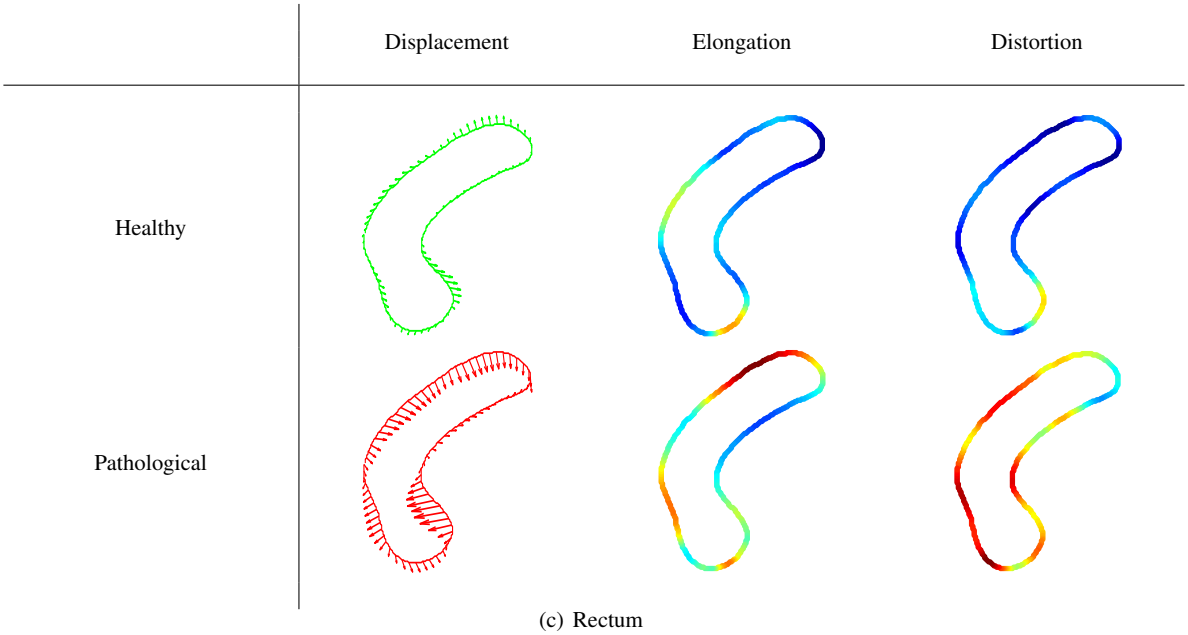

(c) Rectum

Fig. 11 Results of the principal displacement and deformation mode, computed on the healthy and the pathological cases of the three pelvic organs.

organs, the local analysis delimited the non-homogeneous sectors in a way which has a clinical meaning.

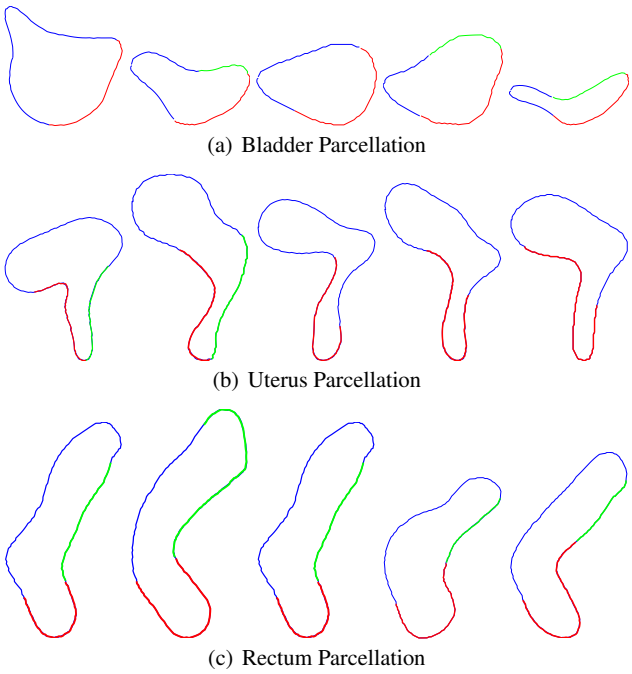

(a) Bladder Parcellation

(b) Uterus Parcellation

(c) Rectum Parcellation

Fig. 12 Some results of the organ parcellation.

5 Conclusion

In this paper, we present a methodological framework based on the use of the current representation of curves. It is based on the LDDMM associated with mechanical deformation features. We applied this methodological framework to the specific case implying the pelvic organs but we believe that it could be successfully employed with any study related to a contour based dynamics characterization. The proposed approach is composed of three stages, which are the mapping, the feature extraction and the analysis. The mapping inter and intra patient uses the LDDMM method, this was performed against a template computed from the available data. The computed template exploits the curve representation based on the currents, and an *anatomically coherent* mean shape is computed. It allowed us to solve the problem of the lack and the mobility of the anatomical landmarks, and also the problem of the large morphological differences between the soft-tissue structures.

The methodology is applied to build a quantitative characterization of the pelvic organ dynamics, in order to have a better pathophysiology understanding. The extracted features quantify the deformations of the organs at each contour point. They describe the displacements of the organ, but also mechanics related measurements (elongation, distortion). They will be a key feature for the validation of the biomechanical behavior laws of the pelvic organs, used in numerical simulations [5]. Indeed, we are able to compare local organ deformations observed with the dynamic MRI to the simulated ones.

Then, the inter-subject analysis of the deformation features helped to distinguish pathological cases from healthy ones. This result validates the relevance of the features chosen for the pelvic dynamics assessment. A study on a larger dataset of MRI sequences would bring a quantitative assessment of the feature, and would open the possibility to build a diagnosis-aid system.

Furthermore, we highlighted the principal trends of variations of the pathological and healthy organs available in our database. Those modes are clinically relevant as they are in adequacy with the clinicians observations. Such statistical tools offer a way for classifying new sequences according to their pathologies, age, *etc*. The synthesis of the geometrical variations into the principal modes of variations make easier the identification of spatially correlated anatomical references. Within this context, the local analysis of the pelvic organs highlighted the anisotropic deformation properties of these organs, which cannot be retrieved by common geometrical features, such as the area, the perimeter, *etc*.

As a result of the local analysis, we proposed a parcellation of the organ contour. This parcellation is based on the deformation profiles of the organ points. It provides a delimitation of parcels associated with significant anatomical references. On the whole, the automated results produced are consistent with the clinical experience that shows the soundness of the approach. As perspectives, improvements on the spatial resolution and the frame rate of the dynamic MRI would bring a more precise analysis, such as finding a temporal regression [27], of the organ dynamics during abdominal strains. Interactions between the main pelvic organs may be investigated as well. The implementation of the LDDMM method is not optimized at this time, as the main goal of this work is to study the feasibility of the approach. It would be interesting to work over this matter, in order to develop a practical tool well suited to the clinical context. The stationary LDDMM proposed in [23] could be experimented, as it enhances the computing time. Moreover, in order to have a fully automated process, we are currently working on automating the segmentation process.

Acknowledgements We thank Dr. J. Lefèvre for the fruitful discussions about the LDDMM method.

References

1. Ashburner, J., Friston, K.: Voxel-based morphometry–the methods. Neuroimage **11**(6), 805–821 (2000)

2. Auzias, G., Colliot, O., Glaunes, J., Perrot, M., Mangin, J.F., Trouvé, A., Baillet, S.: Diffeomorphic brain registration under exhaustive sulcal constraints. IEEE Trans. Med. Imaging **30**(6), 1214–1227 (2011)
3. Ball, G., Hall, D.: A clustering technique for summarizing multivariate data. Behavioral Science **12**(2), 153–155 (1967)
4. Beg, M., Khan, A.: Computing an average anatomical atlas using LDDMM and geodesic shooting. In: IEEE International Symposium on Biomedical Imaging–ISBI 2006, pp. 1116–1119 (2006)
5. Bellemare, M.E., Pirró, N., Marsac, L., Durieux., O.: Toward the simulation of the strain of female pelvic organs. In: IEEE EMBS Annual International Conference, pp. 2756–2759 (2007)
6. Bookstein, F.: Morphometric tools for landmark data: geometry and biology. Cambridge Univ Pr (1997)
7. Chiang, M.C., Dutton, R.A., Hayashi, K.M., Lopez, O.L., Aizenstein, H.J., Toga, A.W., Becker, J.T., Thompson, P.M.: 3d pattern of brain atrophy in hiv/aids visualized using tensor-based morphometry. NeuroImage **34**(1), 44 – 60 (2007)
8. Constantinou, C., Hvistendahl, G., Ryhammer, A., Nagel, L., Djurhuus, J.: Determining the displacement of the pelvic floor and pelvic organs during voluntary contractions using magnetic resonance imaging in younger and older women. BJU international **90**(4), 408–414 (2002)
9. Cootes, T., Taylor, C.: A mixture model for representing shape variation. Image and Vision Computing **17**(8), 567 – 573 (1999)
10. Cox, T., Cox, M.: Multidimensional scaling. Chapman & Hall/CRC (2001)
11. Crum, W., Hartkens, T., Hill, D.: Non-rigid image registration: theory and practice. British journal of radiology **77**(Special Issue 2), S140 (2004)
12. Dryden, I., Mardia, K.: Statistical shape analysis, vol. 4. John Wiley & Sons Chichester, UK (1998)
13. Dupuis, P. and Grenander, U. and Miller, M.I. and Lefschetz : Variational problems on flows of diffeomorphisms for image matching. Quarterly of applied mathematics **56**(3), 587 (1998)
14. Durrleman, S., Pennec, X., Trouvé, A., Gerig, G., Ayache, N.: Spatiotemporal atlas estimation for developmental delay detection in longitudinal datasets. Medical Image Computing and Computer-Assisted Intervention–MICCAI 2009 pp. 297–304 (2009)
15. Durrleman, S. and Pennec, X. and Trouvé, A. and Thompson, P. and Ayache, N. : Inferring brain variability from diffeomorphic deformations of currents: an integrative approach. Medical image analysis **12**(5), 626–637 (2008)
16. Everitt, B., Landau, S., Leese, M.: Cluster analysis. Arnold (2001)
17. Fielding, J.R.: Mr imaging of pelvic floor relaxation. Radiologic Clinics of North America **41**(4), 747 – 756 (2003)
18. Fox, N., Cousens, S., Scahill, R., Harvey, R., Rossor, M.: Using serial registered brain magnetic resonance imaging to measure disease progression in alzheimer disease: power calculations and estimates of sample size to detect treatment effects. Archives of neurology **57**(3), 339 (2000)
19. Frey, B.J., Dueck, D.: Clustering by passing messages between data points. Science **315**, 972–976 (2007)
20. Glaunes, J., Qiu, A., Miller, M., Younes, L.: Large deformation diffeomorphic metric curve mapping. Int. journal of computer vision **80**(3), 317–336 (2008)
21. Golland, P., Grimson, W., Kikinis, R.: Statistical shape analysis using fixed topology skeletons: Corpus callosum study. In: Information Processing in Medical Imaging, pp. 382–387. Springer (1999)
22. Harders, M., Székely, G.: Using statistical shape analysis for the determination of uterine deformation states during hydrometra. Medical Image Computing and Computer-Assisted Intervention–MICCAI 2007 pp. 858–865 (2007)
23. Hernandez, M. and Bossa, M.N. and Olmos, S. : Registration of anatomical images using paths of diffeomorphisms parameterized with stationary vector field flows. International journal of computer vision **85**(3), 291–306 (2009)
24. Hurley, J., Cattell, R.: The procrustes program: Producing direct rotation to test a hypothesized factor structure. Behavioral Science **7**(2), 258–262 (1962)
25. Jian, B. and Vemuri, B. : Robust point set registration using gaussian mixture models. Pattern Analysis and Machine Intelligence, IEEE Transactions on **33**(8), 1633–1645 (2011)
26. Joshi, S. and Davis, B. and Jomier, M. and Gerig, G. : Unbiased diffeomorphic atlas construction for computational anatomy. NeuroImage **23**, S151–S160 (2004)
27. Katanoda, K., Matsuda, Y., Sugishita, M.: A spatio-temporal regression model for the analysis of functional mri data. Neuroimage **17**(3), 1415–1428 (2002)
28. Lawrence, J., Lukacz, E., Nager, C., Hsu, J., Luber, K.: Prevalence and co-occurrence of pelvic floor disorders in community-dwelling women. Obstetrics & Gynecology **111**(3), 678 (2008)
29. Lebedev, L., Cloud, M., Eremeyev, V.: Tensor Analysis with Applications in Mechanics. World Scientific Publishing Company (2010)
30. Lepore, N., Brun, C., Chou, Y., Chiang, M., Dutton, R., Hayashi, K., Luders, E., Lopez, O., Aizenstein, H., Toga, A., et al.: Generalized tensor-based morphometry of hiv/aids using multivariate statistics on deformation tensors. Medical Imaging, IEEE Transactions on **27**(1), 129–141 (2008)
31. Lohmann, G.: Eigenshape analysis of microfossils: a general morphometric procedure for describing changes in shape. Mathematical Geology **15**(6), 659–672 (1983)
32. Maher, C., Baessler, K., Glazener, C., Adams, E., Hagen., S.: Surgical management of pelvic organ prolapse in women. Cochrane Database of Systematic Reviews **18**(4) (2004)
33. Maintz, J., Viergever, M.: A survey of medical image registration. Medical image analysis **2**(1), 1–36 (1998)
34. Marsland, S. and Twining, C.J. : Constructing diffeomorphic representations for the groupwise analysis of nonrigid registrations of medical images. Medical Imaging, IEEE Transactions on **23**, 1006–1020 (2004)
35. Noblet, V., Heinrich, C., Heitz, F., Armspach, J.: 3-d deformable image registration: a topology preservation scheme based on hierarchical deformation models and interval analysis optimization. Image Processing, IEEE Transactions on **14**(5), 553–566 (2005)
36. Paragios, N.: A level set approach for shape-driven segmentation and tracking of the left ventricle. Medical Imaging, IEEE Transactions on **22**(6), 773–776 (2003)
37. Rahim, M., Bellemare, M.E., Pirró, N., Bulot, R.: A shape descriptors comparison for organs deformation sequence characterization in mri sequences. In: IEEE International Conference on Image Processing, ICIP 2009, pp. 1069 – 1072 (2009)
38. Seynaeve, R., Billiet, I., Vossaert, P., Verleyen, P., Steegmans, A.: MR imaging of the pelvic floor. JBR-BTR **89**(4), 182–189 (2006)
39. Singh, N. and Fletcher, P. and Preston, J. and Ha, L. and King, R. and Marron, J. and Wiener, M. and Joshi, S. : Multivariate statistical analysis of deformation momenta relating anatomical shape to neuropsychological measures. Medical Image Computing and Computer-Assisted Intervention–MICCAI 2010, 529–537 (2010)
40. Slieker-ten Hove, M., Pool-Goudzwaard, A., Eijkemans, M., Steegers-Theunissen, R., Burger, C., Vierhout, M.: Prediction model and prognostic index to estimate clinically relevant pelvic organ prolapse in a general female population. International Urogynecology Journal **20**, 1013–1021 (2009)
41. Thomaz, C., Duran, F., Busatto, G., Gillies, D., Rueckert, D.: Multivariate statistical differences of mri samples of the human brain. Journal of Mathematical Imaging and Vision **29**, 95–106 (2007)
42. Weber, A.M., Richter, H.E.: Pelvic organ prolapse. Obstetrics and Gynecology **106**(3), 615–634 (2005)